applied sciences

MDPI

Article

Optimization Design of RC Elevated Water Tanks under Seismic Loads

Francisco J. Martínez-Martín [1], Víctor Yepes [2,*], Fernando González-Vidosa [2], Antonio Hospitaler [2] and Julián Alcalá [2]

[1] Tecozam Estructuras y Drenajes SL, 28036 Madrid, Spain; franciscoj.martinez@tecozam.com
[2] Institute of Concrete Science and Technology (ICITECH), Universitat Politècnica de València, 46022 Valencia, Spain; fgonzale@cst.upv.es (F.G.-V.); ahospitaler@upv.es (A.H.); jualgon@cst.upv.es (J.A.)
* Correspondence: vyepesp@cst.upv.es; Tel.: +34-96-387-9563

Abstract: This paper deals with the seismic column design of 35 elevated RC water storage tanks. Tanks comprise a top conic trunk reservoir, a column with variable hollow square cross-sections, and a shallow foundation on a sand layer. The five-column heights considered are 20, 25, 30, 35, and 40 m. The five tanks are subjected to seven degrees of seismic loading characterized by the reference peak ground acceleration in Eurocode 8. The elevated tanks are designed against the full prescriptions of Eurocode 2, Eurocode 8, and the Spaniard Structural Code of Practice. This includes variable loads for seismicity, wind, snow, etc., together with the action of self-weight and dead loads. The optimization design method considered is a variant of the old bachelor algorithm, an adaptive threshold acceptance method with a neighborhood move based on the mutation operator from genetic algorithms. Column results show the high nonlinearity of the problem since the horizontal seismic forces depend on the rigidity and height of the columns. The main features of the optimized tanks give guidance for the practical design of this kind of elevated RC water tank.

Keywords: concrete structures; economic optimization; elevated water tanks; old bachelor algorithm; seismic loading; structural design

Citation: Martínez-Martín, F.J.; Yepes, V.; González-Vidosa, F.; Hospitaler, A.; Alcalá, J. Optimization Design of RC Elevated Water Tanks under Seismic Loads. *Appl. Sci.* **2022**, *12*, 5635. https://doi.org/10.3390/app12115635

Academic Editor: Dario De Domenico

Received: 12 May 2022
Accepted: 31 May 2022
Published: 1 June 2022

1. Introduction

Elevated tanks are critical structures in water supply networks. These tank facilities are usually located on tall structures that provide sufficient pressure for water distribution systems. Tanks also serve for storage that covers possible interruptions in the pumping system. Thus, this structure is essential for public services and there is a vital need for it to remain operational after severe earthquakes. The poor seismic performance of these inverted pendulum-type constructions are frequently reported during major earthquakes [1–4]. The seismic response of concrete and steel tanks was extensively investigated through experimental and numerical methods [5–8]. Factors that affect the seismic response of tanks include the tank size [9], the soil–structure interaction [10], and the fluid–structure interaction [11]. Regarding the optimized design of elevated RC water tanks, to the best of the authors' knowledge, there was no research conducted to date.

Structural engineering aims to achieve maximum safety with minimum investment. This target is not easy as long as various design variables with multiple combinations characterize structural problems. Researchers have explored new ways to achieve structural efficiency. In conjunction with evolutionary-based optimization procedures, finite element modeling techniques were used to design conical steel water tanks on elevated towers [12] and rectangular RC reservoirs [13]. However, most of the approaches found in the literature were not suitable to be implemented in real-life structures [14]. Much research was conducted recently concerning metaheuristics applied to structural optimization, such as metasimulated annealing and metathreshold accepting [15], harmony search [16–18], swarm intelligence methods [19,20], and biogeography-based optimization [21], among others.

Models without physical meaning or without being based on nature can also be used in structural optimization, as in the case of machine learning algorithms [22]. Since machine learning models do not have a physical meaning, further study and deepening of the model output are necessary. Once a model is calibrated, the next step is to find the main patterns and variables that explain this model. Analyzing the variables makes it possible to understand the correlation between them and associate this correlation with an expert meaning that comes from a physical model or an expert in the area. These machine learning models allow for understanding or eliminating specific patterns or relationships that the model has found. On the other hand, when these conditions are found, they can be introduced as a physical constraint to calibrate the model [23,24]. The results obtained in the structural design case can be used to analyze the variables that have the most significant impact on the design, the values they take, and their relationship. Subsequently, it is possible to identify which physical condition sustains these relationships.

This paper employs the hybridization strategy to combine the strengths of individual algorithms and exploit the complementary character of different optimization strategies. Lopes Silva et al. [25] provided a survey on the hybridization of metaheuristics with other techniques for optimization problems. In this context, these techniques proved the efficiency of threshold accepting-based techniques to optimize bridge piers [26], post-tensioned concrete box girder bridges [27], and wind turbine foundations [28].

Following this line of work, this paper focuses on the economic seismic optimization of columns for elevated concrete water storage conical tanks. To this end, a Fortran program encompasses modules for structural analysis, limit states verification, and cost evaluation. A hybrid threshold acceptance adaptive algorithm with a mutation operator (abbreviated herein as OBAMO) was then used to search the solution space in order to identify a set of solutions with optimized values for the designer. The study shows the algorithm's applicability to the structure and provides engineers with guidelines for efficient design.

2. Optimization Problem Definition

2.1. Elevated Water Tanks Object of Optimization

The RC elevated water tanks consist of a high reservoir of conic trunk shape, a column with a hollow square cross-section, and a footing as a shallow foundation (Figures 1 and 2). The top reservoir keeps a constant geometry and steel reinforcement for the water tanks considered in the study. The top reservoir was analyzed by SAP2000 using two-dimensional shell finite elements of four nodes, whose parameters are the element thickness, together with the Young modulus, and the Poisson's ratio of the material. Alternative methods to the finite element method are the finite difference method [29] and the discrete element method [30]. Given the stress resultants, the reinforcement of the reservoir was computed by Eurocode 2 [31] and the Spaniard Code of Structures [32]. Figures 3–5 show the final reinforcement. The height of the conic trunk reservoir is 6 m, and the outer and inner diameters are 14 and 7 m, respectively. Man access of 1.20 m in diameter with walls of 0.20 m of thickness crosses the reservoir. This access goes from the column shaft to the top platform of the reservoir. The tank also has a handrail that surrounds the top slab. All the reservoir walls have a thickness of 0.30 m in concrete class C-30. The reservoir volume is 533.08 m^3, excluding the man's access.

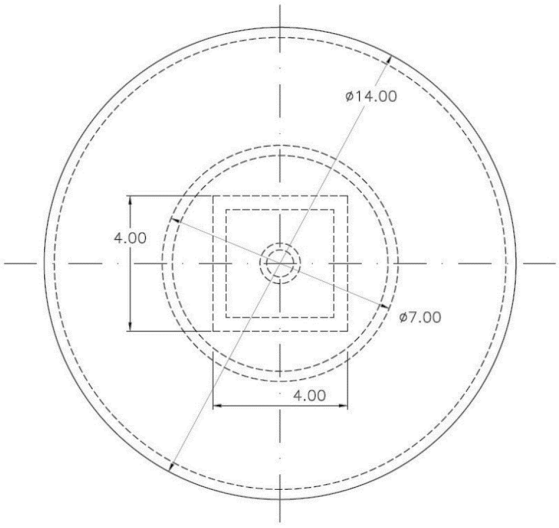

Figure 1. Typical plan view of an elevated water tank.

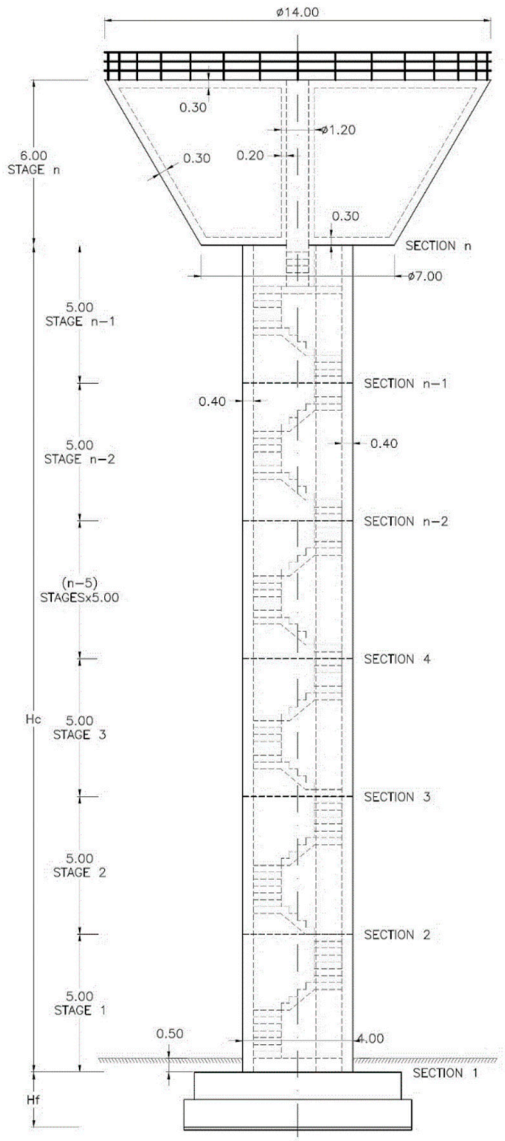

Figure 2. Typical elevation of an elevated water tank.

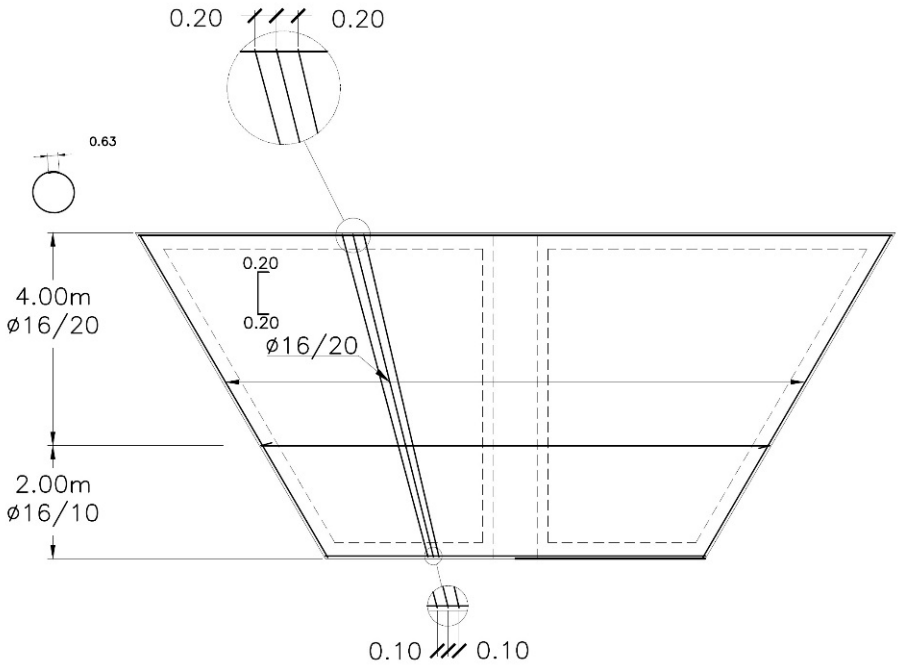

Figure 3. Steel reinforcement elevation of the reservoir.

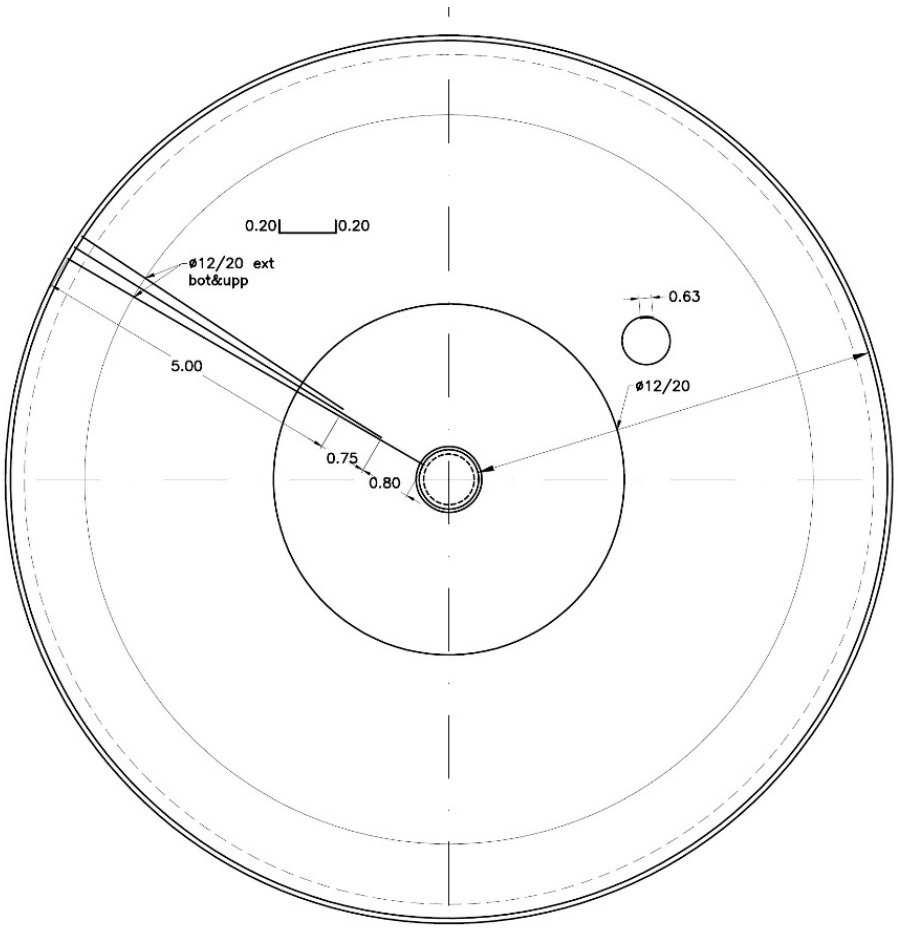

Figure 4. Reinforcement plan view of the top slab of the reservoir.

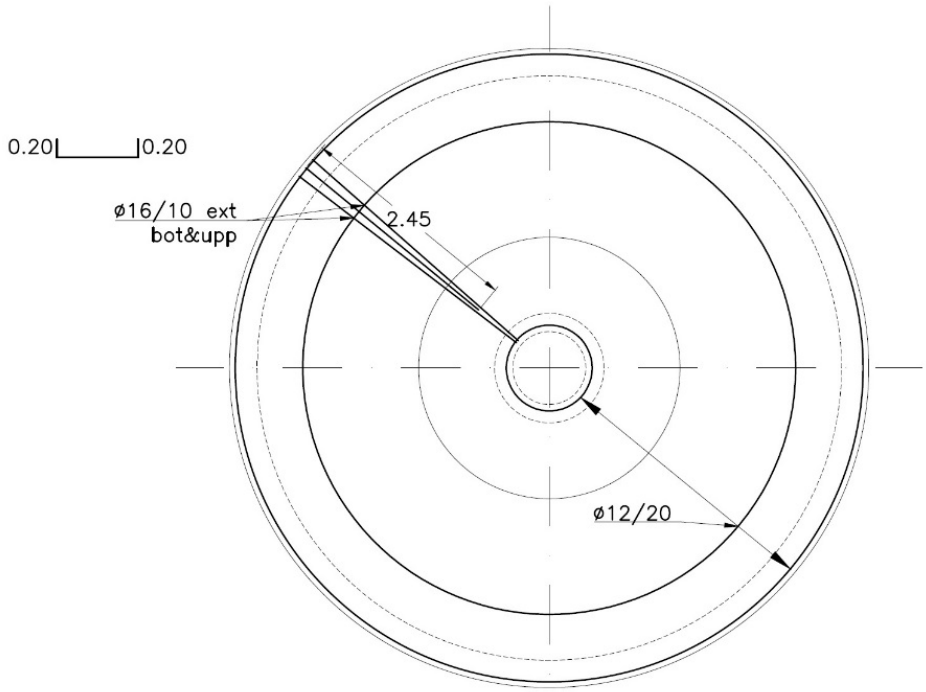

Figure 5. Reinforcement plan view of the bottom slab of the reservoir.

An RC column supports the reservoir with square hollow sections founded on a footing (Figure 2). The column and the footing are optimized regarding their geometry and the steel reinforcement. The height and the cross-sections of the column play a key role in the structure's stiffness, which is crucial for the external forces and the stress resultants caused by earthquakes. Note that the present paper concentrates on the design interaction of the seismic action with the column's height and rigidity. This highly nonlinear problem is studied for a constant top reservoir. First and second-order stress resultants of the one-degree freedom oscillator are computed directly without any finite element simulation. The analysis considers five-column heights, from 20 to 40 m in steps of 5 m (Figure 2). Column stretches are defined by the variables that determine their cross-section, the concrete quality, and the steel reinforcement. The characteristics of each stretch are doubly symmetric since the seismic actions considered can act in any positive or negative direction (Figure 6). Index *i* in Figure 6 indicates a given column stretch since the wall thicknesses, reinforcement, and concrete quality can vary in each stretch. The external width of the column is a geometric variable that can vary between 1.80 and 4.90 m in steps of 0.10 m. This width is constant at the full height of the column. The limit of 4.90 is that of the size of the square inscribed in a circle of 7.00 m, which corresponds with the bottom dimension of the reservoir. The thickness of the column walls can vary in the different stretches, with a minimum of 0.25 m and a maximum of 0.75 m in steps of 2.5 cm. It is required that the thickness of the walls either keeps constant or reduces in height. The vertical reinforcement is placed in the outer and inner faces of the column. The number and diameter of the bars in each face define it. The vertical bars of the first stretch faces could be spaced between 0.100 and 0.300 m in steps of 2 mm. This gives 101 spacing possibilities. A given stretch face of the column can keep the number of bars in the stretch below or reduce it to half (half plus one bar if the number of bars in the stretch below is odd) unless the resulting spacing between bars would exceed 0.30 m. The possible diameters of the bars are 12, 16, 20, 25, and 32 mm. In addition, the diameter of the bars in a given stretch face cannot be larger than that of the stretch below. The vertical bars are kept in place through small horizontal stirrups with a minimum diameter of 8 mm for assembly. More oversized stirrups from one external face to the opposite external face serve as shear reinforcement with diameters of 12, 16, or 20 mm spacing between 0.100 and 0.300 m in steps of 2.5 mm. A given stretch cannot

have stirrups of greater diameter or spaced less than the stretch below. This is following the reduction in the height of the stress resultants. Concrete strength qualities can be those of C-25, C-30, C-35, C-40, and C-45, where the number is f_{ck} in MPa, i.e., the compressive characteristic cylinder strength at 28 days. The concrete strength of a given stretch has to be equal to or smaller than that of the stretch below.

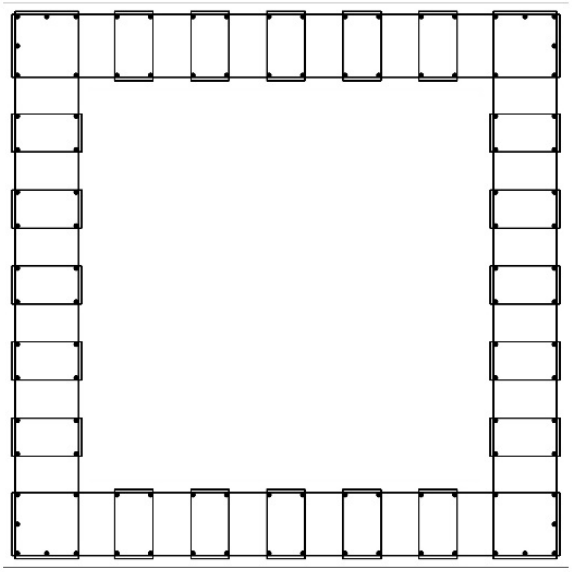

Figure 6. Typical cross section of the column.

The foundation was considered shallow, formed by a doubly symmetric footing in both geometry and steel reinforcement (Figure 7). This foundation is made of a bottom footing and a plinth. The total foundation depth varies from 1.00 to 4.00 m in steps of 0.10 m. The total depth is split into two equal parts so that the bottom footing and the plinth have the same depth. The plan dimensions of the plinth are imposed to be greater than the width of the column plus the depth of the footing. The plan dimensions of the plinth should be smaller than those of the bottom footing. Both the dimensions of the plinth and the bottom footing can vary from a minimum of 4.00 m to a maximum of 15.00 m in steps of 0.25 m. Concrete quality in the foundation is the same as for the column, following the sequence C-25, C-30, C-35, C-40, and C-45. The main reinforcement of the foundation is the bottom layers of steel. Reinforcement is made of up to four layers. The possible diameters of the bars are 12, 16, 20, 25, and 32 mm. Spacing can vary from 0.100 m to 0.300 m in steps of 2.5 mm.

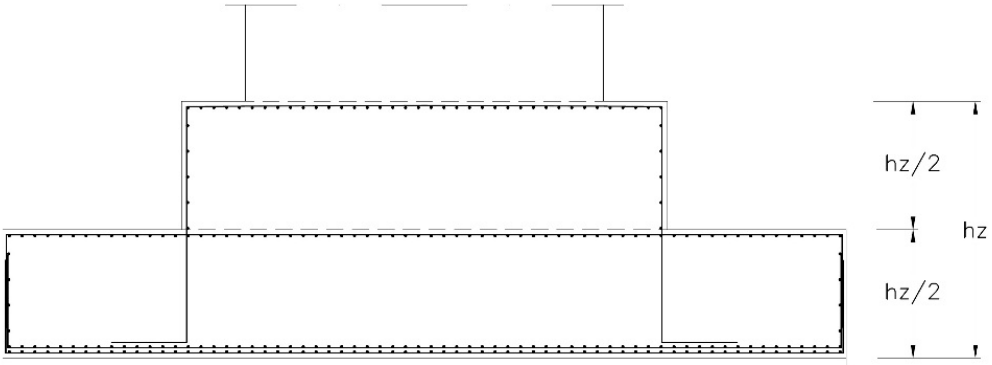

Figure 7. Cross section of the footing foundation.

2.2. Problem Definition

The problem consists of the cost of the design optimization of an elevated RC water tank regarding its column and its foundation, the reservoir being constant during the optimization analysis. The study aims to minimize the cost of the objective function F in Equation (1) while satisfying the structural restrictions of the problem in Equation (2). Possible values of the $x_1, x_2, \ldots, x_n$ design variables are given in Equation (3).

$$F(x_1, x_2, \ldots, x_n) = \sum_{i=1,r} p_i * m_i(x_1, x_2, \ldots, x_n) \quad (1)$$

$$g_j(x_1, x_2, \ldots, x_n) \leq 0 \quad (2)$$

$$x_i \in (d_{i1}, d_{i2}, \ldots, d_{iq}) \quad (3)$$

In addition, the structure has to comply with the structural constraints. All variables are discrete in the present model since one of the objectives of the study is that the resulting structure is fully defined and constructible. The rest of the necessary values to define the structure are the parameters. The main parameters are the height of the column of the water tank and the seismic action considered. The geometrical parameters are the shape and dimensions of the reservoir (533.08 m^3), the height of the column, and the 5 m height of the climbing form. The height of the column varies from 20 to 40 m in steps of 5 m. The main seismic parameters are the reference peak ground accelerations considered, a_{gR}, which are from 0.00g to 0.24g in steps of 0.04g, where g is the gravity acceleration. Ground parameters are the density of the fill on top of the footing, the internal friction angle of the founding sands, the SPT of the founding sands, and the friction angle between the footing and the ground (Table 1). Steel reinforcement parameters are the f_{yk} = 500 MPa type of steel and the reinforcement of the lateral faces of the footing and plinth (Ø12/20). Water tanks were analyzed in full compliance with the normative codes [31–34]. Finally, there are parameters for the ambient exposure of the different elements: internal, external, and buried.

Table 1. Basic parameters of geometry and foundation ground.

Parameter	Value
Height of column formworks	5.00 m
Internal friction angle of the sands	35°
Standard penetration test (SPT) sands	30
Ground– footing friction angle	30°
Specific weight of the ground	20.00 kN/m^3

The objective function in Equation (1) is the total cost of the water tank, where p_i are the unit prices and m_i are the measurements of the different units. The cost of each unit is obtained by multiplying the unit price by the measurement. Unit prices are summarized in Tables 2–4. Each concrete mix can be obtained with different water/cement ratios, kilograms of cement per cubic meter, and consistency measured by the Abrams cone, which can be plastic or flabby. All these concrete mix properties affect the verification of the durability constraints.

Table 2. Unit costs.

Unit	Cost (€/Unit)
kg steel reinforcement in columns (f_{yk} = 500)s	1.99
kg steel reinforcement in footing (f_{yk} = 500)	1.07
m^2 formwork in footing	18.19
m^2 external formwork in columns	48.19
m^2 internal formwork in columns	49.50
m^3 concrete pumped placing in column	26.03
m^3 concrete not pumped placing in column	27.34
m^3 concrete not pumped placing in footing	12.74
m^3 excavation	9.42
m^3 earth fill	4.81

Table 3. Concrete unit costs for C-25 and C-30.

Concrete Type	Water/Cement	Cement (kg)	Slump	Cost (€/m^3)
C-25(1)	0.65	250	Flabby	70.79
C-25(2)	0.60	275	Flabby	72.78
C-25(3)	0.60	300	Flabby	73.93
C-25(4)	0.60	325	Flabby	75.49
C-25(5)	0.60	350	Flabby	76.63
C-25(6)	0.65	250	Plastic	69.40
C-25(7)	0.60	275	Plastic	71.35
C-25(8)	0.60	300	Plastic	72.48
C-25(9)	0.60	325	Plastic	74.01
C-25(10)	0.60	350	Plastic	75.12
C-30(1)	0.65	250	Flabby	73.62
C-30(2)	0.60	275	Flabby	75.69
C-30(3)	0.60	300	Flabby	76.89
C-30(4)	0.60	325	Flabby	78.51
C-30(5)	0.60	350	Flabby	79.69
C-30(6)	0.55	300	Flabby	79.66
C-30(7)	0.50	300	Flabby	79.85
C-30(8)	0.50	325	Flabby	82.75
C-30(9)	0.65	250	Plastic	72.18
C-30(10)	0.60	275	Plastic	74.20
C-30(11)	0.60	300	Plastic	75.38
C-30(12)	0.60	325	Plastic	76.97
C-30(13)	0.60	350	Plastic	78.13
C-30(14)	0.55	300	Plastic	78.10
C-30(15)	0.50	300	Plastic	78.29
C-30(16)	0.50	325	Plastic	81.13

Table 4. Concrete unit costs for C-35, C-40 and C-45.

Concrete Type	Water/Cement	Cement (kg)	Slump	Cost (€/m^3)
C-35(1)	0.65	250	Flabby	76.45
C-35(2)	0.60	275	Flabby	78.60
C-35(3)	0.60	300	Flabby	79.85
C-35(4)	0.60	325	Flabby	81.53
C-35(5)	0.60	350	Flabby	82.76
C-35(6)	0.55	300	Flabby	82.80
C-35(7)	0.50	300	Flabby	82.92
C-35(8)	0.50	325	Flabby	85.93
C-35(9)	0.45	350	Flabby	88.72
C-35(10)	0.65	250	Plastic	74.95
C-35(11)	0.60	275	Plastic	77.06
C-35(12)	0.60	300	Plastic	78.28
C-35(13)	0.60	325	Plastic	79.93
C-35(14)	0.60	350	Plastic	81.13
C-35(15)	0.55	300	Plastic	81.20
C-35(16)	0.50	300	Plastic	81.30
C-35(17)	0.50	325	Plastic	84.25
C-35(18)	0.45	350	Plastic	86.98
C-40(1)	0.50	300	Flabby	85.99
C-40(2)	0.50	325	Flabby	89.12
C-40(3)	0.45	350	Flabby	92.00
C-40(4)	0.50	300	Plastic	84.31
C-40(5)	0.50	325	Plastic	87.37
C-40(6)	0.45	350	Plastic	90.20
C-45(1)	0.50	300	Flabby	89.07
C-45(2)	0.50	325	Flabby	92.30
C-45(3)	0.45	350	Flabby	92.00
C-45(4)	0.50	300	Plastic	87.32
C-45(5)	0.50	325	Plastic	90.49
C-45(6)	0.45	350	Plastic	93.42

The constraints of the problem are related to the serviceability of the structure, together with ultimate limit states of stability and strength. They are the service and ultimate limit states that must fulfill the reservoir, the column, and the foundation for all the combinations of actions according to Eurocode 2 [31] and the Spaniard Code of Structures [32]. Additionally, the problem has implicit constraints regarding geometry, steel reinforcement, materials, and constructability.

Actions were considered following Eurocode 1 [35] and the Basic Document SE-AE/CTE [34]. Variable actions include snow on the top slab of the reservoir, wind, and accidental seismic action. Variable actions also include the water in the reservoir, considering that the reservoir can be full or empty. The water tank was modelled as one degree of the freedom-free oscillator. The static equivalent seismic force applied at the center of gravity of the tank was computed. This equivalent seismic force was updated for each iteration of the analyses of the structures being optimized. Two methods were used. First, was the method described by Eurocode 8 [33], and second, was the simplified method by Housner [5]. The present study applies the maximum force computed by the two methods.

The column must comply with the ULS for buckling, shear, and fatigue, as well as the SLS for cracking. The column must also exceed the geometrical and mechanical reinforcement minimums. The bottom and top extremes of these stretches are the basic sections for the analysis of the column. Such cross sections are taken to compute the ULS and SLS, except for the ULS for buckling, which requires a global check. The ULS for buckling requires most of the computational effort due to the great number of iterative checks required.

Regarding the foundation, the geometry is first checked for ground stress limitations. The permissibility of the stress depends on the shape and dimensions of the footing. The

foundation ground is a layer of sands. The internal friction angle of the sands is 35°, and their cohesion is zero. The density of the sands is 2000 kg/m^3, and they have an SPT of 30. The water table is sufficiently deep so as not to affect the foundation. The permissible stress of the foundation is the minimum value obtained for the collapse load [36,37] and a settlement of 25.4 mm. The collapse load q_h in Equation (4) depends on the shape of the foundation, the eccentricity, and inclination of the load, as well as on the depth of the foundation:

$$q_h = q \cdot N_q \cdot S_q \cdot i_q \cdot d_q + c \cdot N_c \cdot S_c \cdot i_c \cdot d_c + \frac{1}{2} \cdot B \cdot \gamma \cdot N_\gamma \cdot S_\gamma \cdot i_\gamma \cdot d_\gamma \quad (4)$$

where N_q, N_c and N_γ are the capacity of load factors; S_q, S_c, and S_γ are the shape factors; i_q, i_c, and i_γ are the inclination factors; d_q, d_c and d_γ are the depth factors; q is the stress on the foundation face prior to the execution of the footing; B is the width of the footing; and γ is the ground density.

The settlement stress S is the stress that produces a maximum settlement of 25.4 mm. It is computed using Equation (5) [38] for granular grounds with a proportion in weight of particles coarser than 20 mm higher than 30%.

$$S = f_l \cdot f_s \cdot q_b \cdot B^{0.7} \cdot I_c \quad (5)$$

where S is the settlement, f_l is a correction factor that takes into account the existence of a rigid layer at a low depth under the footing, f_s is a coefficient that depends on the shape of the footing, q_b is the applied pressure at the foundation face required to cause the settlement S, and I_c is the compressibility index based on the SPT value.

Once the footing is checked for the two permissible stresses, the footing is checked against sliding and overturning. Sliding is checked considering a friction angle between the footing and the ground of 30° and a zero cohesion. This check is given by Equation (6):

$$F_s T \leq N \cdot tg\varphi + c \cdot B \quad (6)$$

where the applied horizontal force T multiplied by the sliding safety coefficient, F_s must be less than or equal to that resistance to slipping given by the product of the normal force N by the tangent of the friction angle plus the cohesion c multiplied by the width of the footing B.

The check on overturning considers that division between the stabilizing moments and the overturning is greater than the safety coefficient. This check is given by Equation (7), where F_v is the overturning safety coefficient.

$$F_v = \frac{\sum stabiliz}{\sum M_{overturn}} \quad (7)$$

Once the geometry of the footing is checked, the ULS of shear, flexure, and fatigue, and the SLS of cracking are checked, as well as the geometrical and mechanical minimum values. The method used for integrating sections is that proposed by Bonet et al. [39], which performs the integration of stresses by the Gauss–Legendre quadrature.

3. Optimization Method

The method of optimization proposed is a hybrid old bachelor algorithm (OBA) [40] with a mutation operator (OBAMO). OBA presents one of its advantages: the user determines the number of iterations. In addition, Agur et al. [41] proved that OBA is a less demanding method from the point of view of computational effort than other traditional metaheuristics such as simulated annealing or threshold accepting. The reason for using this algorithm is that similar algorithms have been used and have given good results in other structural problems [42,43].

This dynamic algorithm varies the acceptance threshold of new solutions as a function of previously accepted solutions. A new solution is accepted when its cost in Equation (8)

($\cos t_{ns}$) is smaller than the cost of the previous solution ($\cos t_{ps}$) and a specific parameter called threshold (U_f). The process is updated, and the new solution becomes the previous solution.

$$\cos t_{ns} < \cos t_{ps} + U_f \tag{8}$$

If the new solution does not meet the condition in Equation (8), then the solution is not accepted and the cost threshold value is increased to the value given in Equation (9):

$$U_f = U_0 + (1000/100) \cdot \left(1 - \left(\frac{p}{2 \cdot sol}\right)\right) \tag{9}$$

where U_f is the new threshold, U_0 is the previous threshold, p is the number of solutions accepted in the searching process, and *sol* is the total number of feasible solutions considered, which in our case is taken as 1000. If the solution is accepted, then the threshold is reduced following Equation (10):

$$U_f = U_0 - count \cdot \left(1 - \left(\frac{p}{sol}\right)\right) \tag{10}$$

where *count* is a counter that considers whether new solutions are found in the search process in less than a certain number of iterations. The counter is added in 1 when the number of iterations to find a new solution is less than 100. The counter is set equal to 1 when the number of iterations to find new solutions is larger than 100. The number of feasible solutions that improve cost plus threshold equals 1000 per computer run. The total number of computer runs equals 25 for each of the 35 water tanks analyzed. This involves 875 computer runs for the whole parametric study in the present paper.

On the other hand, genetic algorithms (GAs) explore the solution space using a population of solutions and operators such as selection, crossover, and mutation. It has implemented a hybrid strategy that combines the synergy effect between the GA and SA [44,45], obtaining encouraging results. The idea is to employ OBA with a neighborhood move based on the mutation operator from the GA; thus, the current solution is changed by a small random change in the values of the variables. These small random variations were selected to avoid random searches in the solution space, and they are justified for practical and constructive processes.

4. Numerical Results

This section presents and discusses the results for the 35 water tanks analyzed. As explained above, the five heights of the column vary from 20 to 40 m in steps of 5 m. Seven seismic exposures are considered characterized by a_{gR}/g from 0.00 to 0.24 in steps of 0.04. Results depend on the numerical nonlinearity of the seismic applied loads, which is the dominant condition in most cases studied. Table 5 shows the equivalent static force due to the seism with the tank full of water. This seismic hypothesis is the most relevant hypothesis for the check of the water tank using Eurocode 8 [33] and the approximate method by Housner [5]. Figure 8 represents these forces and shows the high nonlinearity of the problem and the dependence of the force on the rigidity of the columns. Elevated water tanks have lower rigidity, and hence the seismic force is lower than those of the shorter water tanks. This implies that section and steel reinforcement results are not proportional to the height of the columns, as already observed in the study of seismic viaduct piers by Martínez-Martín et al. [46]. Regarding the value of a_{gR}/g, larger values imply larger equivalent static forces.

Table 5. Horizontal seismic forces (kN).

Column Height (m)	a_{gR}/g	Euroc. 8 (kN)	Housner (kN)
20	0.00	0.00	0.00
20	0.04	341.90	359.16
20	0.08	1232.35	1210.01
20	0.12	2144.68	2055.94
20	0.16	3479.77	3253.73
20	0.20	4198.74	3923.55
20	0.24	5702.18	5252.09
25	0.00	0.00	0.00
25	0.04	249.65	261.80
25	0.08	980.62	996.25
25	0.12	1344.01	1376.53
25	0.16	2245.38	2209.03
25	0.20	3468.79	3305.40
25	0.24	3477.36	3367.75
30	0.00	0.00	0.00
30	0.04	171.02	219.44
30	0.08	602.54	617.07
30	0.12	1568.58	1568.41
30	0.16	1694.09	1739.40
30	0.20	2049.89	2101.60
30	0.24	3082.29	3033.61
35	0.00	0.00	0.00
35	0.04	110.95	161.97
35	0.08	434.30	494.77
35	0.12	824.62	824.61
35	0.16	1356.35	1426.94
35	0.20	1661.61	1746.68
35	0.24	2063.15	2155.73
40	0.00	0.00	0.00
40	0.04	108.76	159.40
40	0.08	345.11	440.62
40	0.12	666.97	732.58
40	0.16	1153.28	1194.16
40	0.20	1390.90	1442.49
40	0.24	1707.13	1790.73

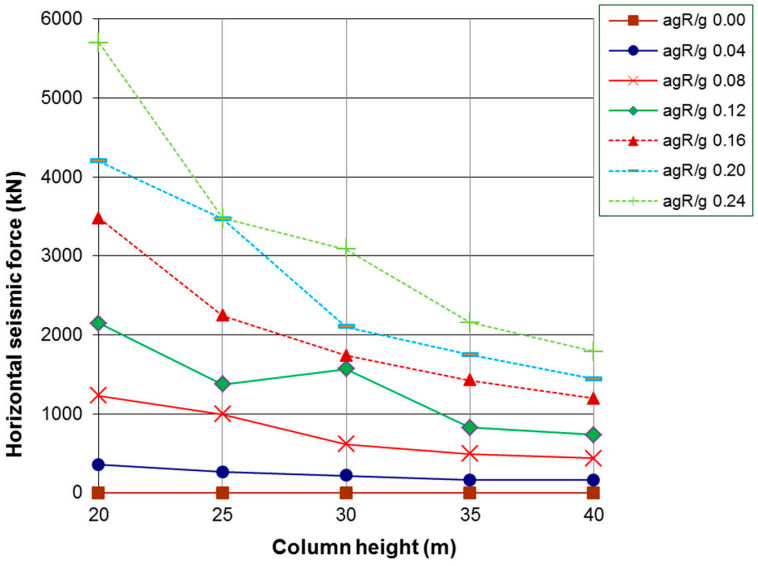

Figure 8. Horizontal seismic force versus height of the column.

Figure 9 illustrates the variation of total concrete volume in the column for different heights and seismic exposures. It shows that concrete values increase with the height of the column and with the seismic degree of force. This measurement of concrete varies from a minimum of 170 m^3 to a maximum of 300 m^3. Figure 10 shows the measurement of steel reinforcement per meter of a column, which varies between 100 kg/m to a maximum of 700 kg/m. This graphic shows a linear increase in steel measurement with the column's height for water tanks not subjected to seismic loads. However, the measurement of steel remains quite the same as the height for water tanks subjected to the same seismic condition.

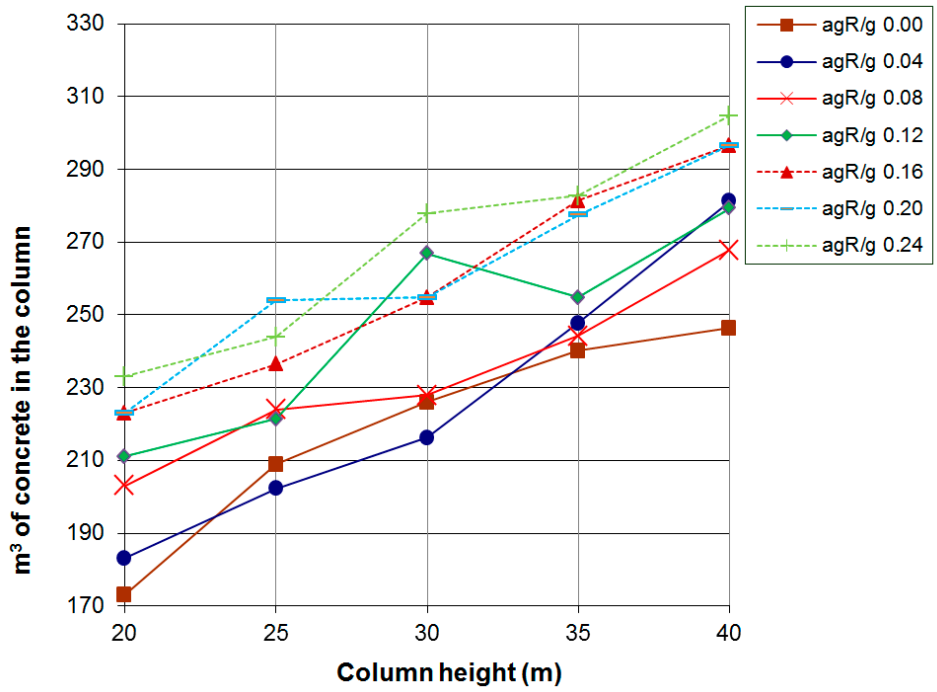

Figure 9. m^3 of concrete in the column versus height of the column.

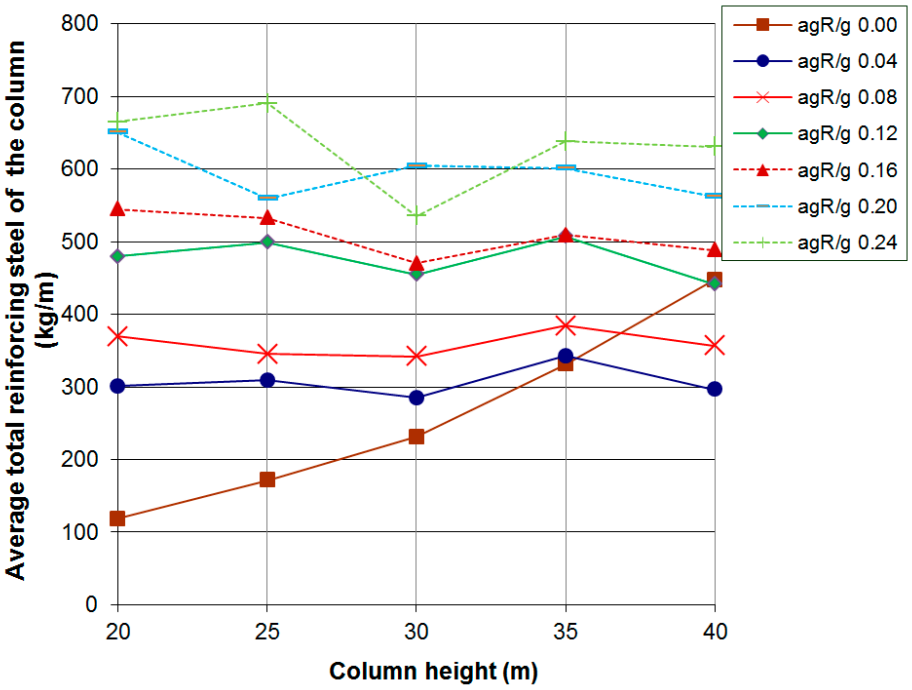

Figure 10. Steel kg/m in the column versus height of the column.

The width is one of the main geometrical variables of the optimization process. Figure 11 shows the column's width versus the column's height. The width of the column varies from a minimum of about 1.75 m to a maximum of about 4.75 m. Although the figure shows some peak values for the water tanks with large seismicity, the overall tendency is that the width of the column for the optimal tank is similar for the different heights studied given seismicity.

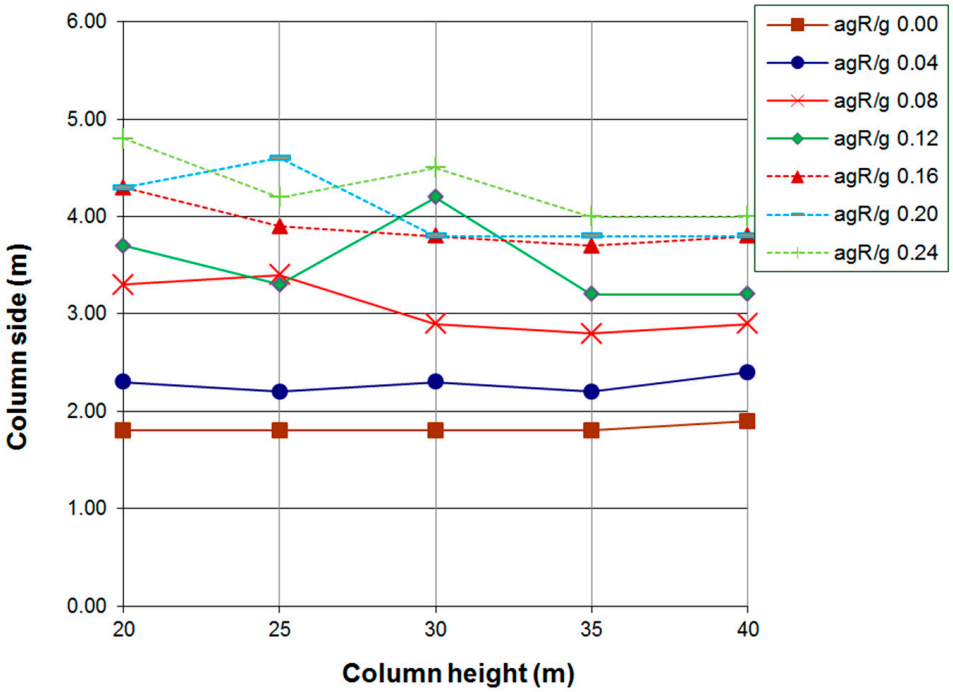

Figure 11. Width of the column versus height of the column.

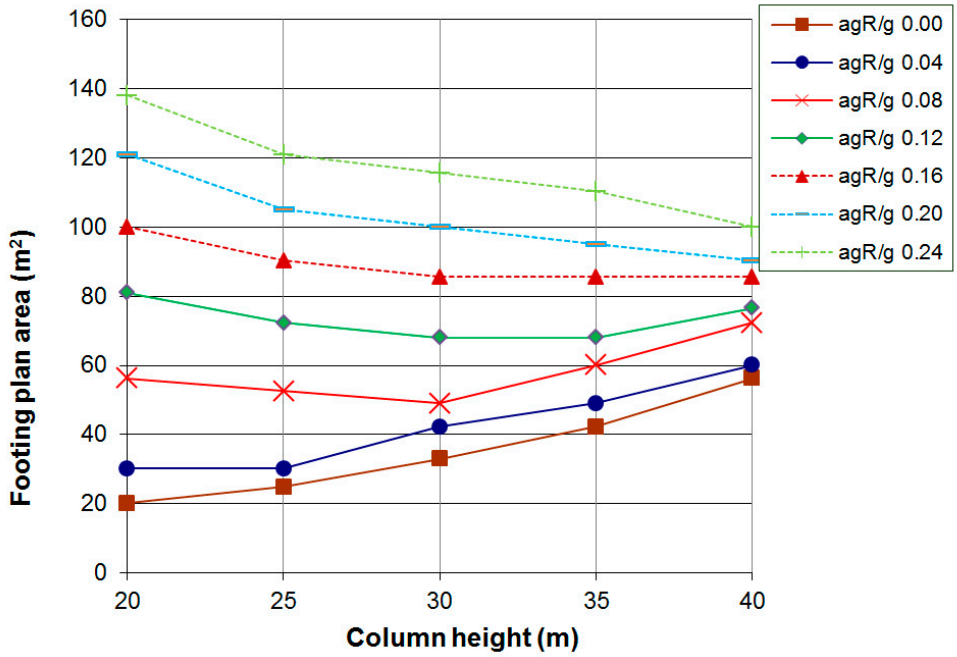

Figure 12. Area of the footing versus height of the column.

Figure 12 shows the total area of the foundation as a function of column height and ground acceleration. This area varies from a minimum of about 20 m^2 for the lowest seismicity to a maximum of about 140 m^2 for the largest seismicity. Figure 13 shows the

total volume of concrete in m^3 in the foundation. The volume of concrete varies from a minimum of about 20 m^3 to a maximum of about 240 m^3. These two graphics can be divided into three result groups. The tendency in the group for a_{gR}/g from 0.00 and 0.08 is that the area of the foundation and the volume of concrete increase notably with the height of the water tank. The group for a_{gR}/g equal to 0.12 keeps sensibly constant the foundation area and the volume of concrete. Finally, the group for a_{gR}/g of 0.16, 0.20, and 0.24 shows a tendency to reduce the foundation area and the volume of concrete with the height of the water tank. It is worth noting that the results are highly nonlinear with the height of the column and the seismicity. Consider that taller columns are more flexible, which reduces the column stress resultants due to ground acceleration. Figure 14 shows the total steel reinforcement in kg in the footing, which varies from a minimum of about 2000 kg to a maximum of about 14,000 kg. Again, the results can be divided into the same three groups with the same tendencies as Figures 12 and 13.

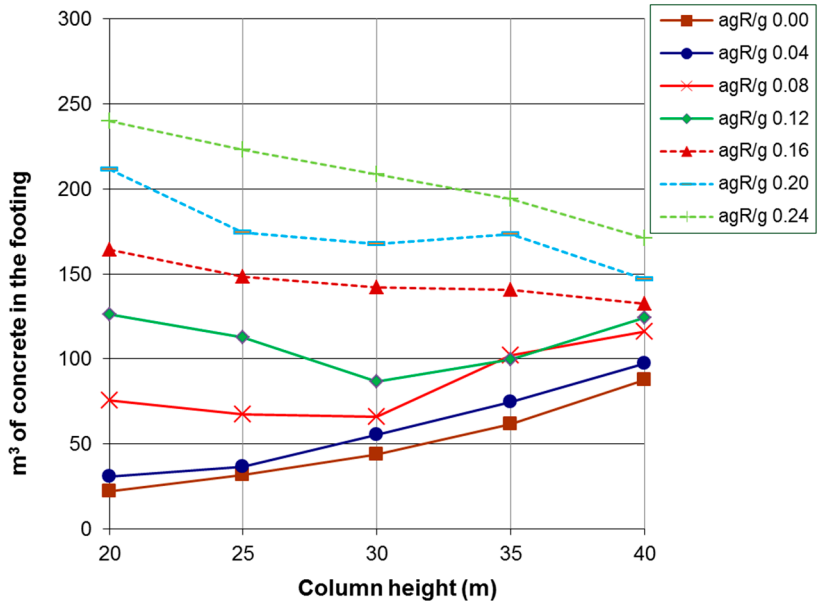

Figure 13. Footing volume of concrete versus height of the column.

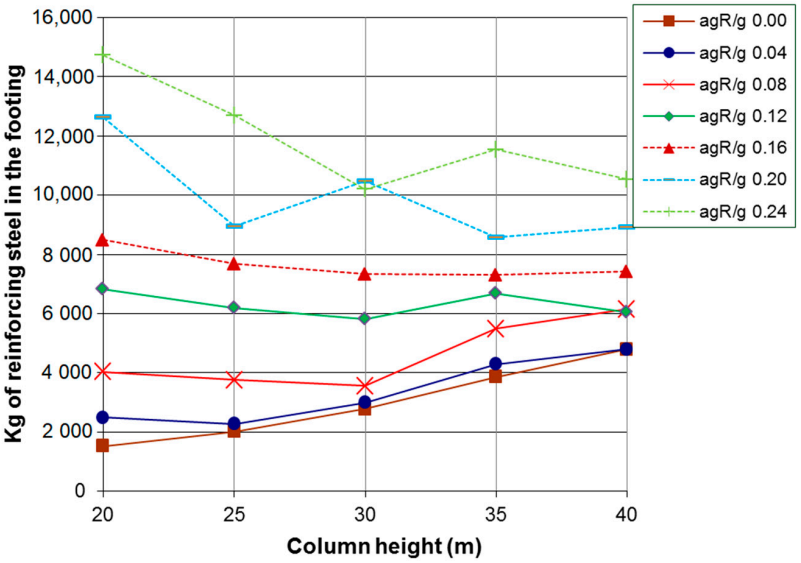

Figure 14. Steel reinforcement in the footing versus height of the column.

Figure 15 shows the total amount of steel in the water tank per meter of the height of the column in kg/m. These values vary from a minimum of about 900 kg/m to a maximum of about 2200 kg/m. Figure 16 shows the total volume of concrete in the water tank per meter of the height of the column in m^3/m. These values vary from a minimum of about 8 m^3/m to a maximum of about 24 m^3/m. Both figures show the same tendency. The amount of steel per unit column decreases with the height. This reduction is more accentuated for larger seismic degrees and shorter heights of the water tanks. Graphs tend to be horizontal when the seismic degree is low and the height of the tanks increases. All of this stresses the high nonlinearity of the problem since taller columns are more flexible and better accommodate the seismic response. Steel reinforcement directly depends on the equivalent seismic force of each of the 35 cases.

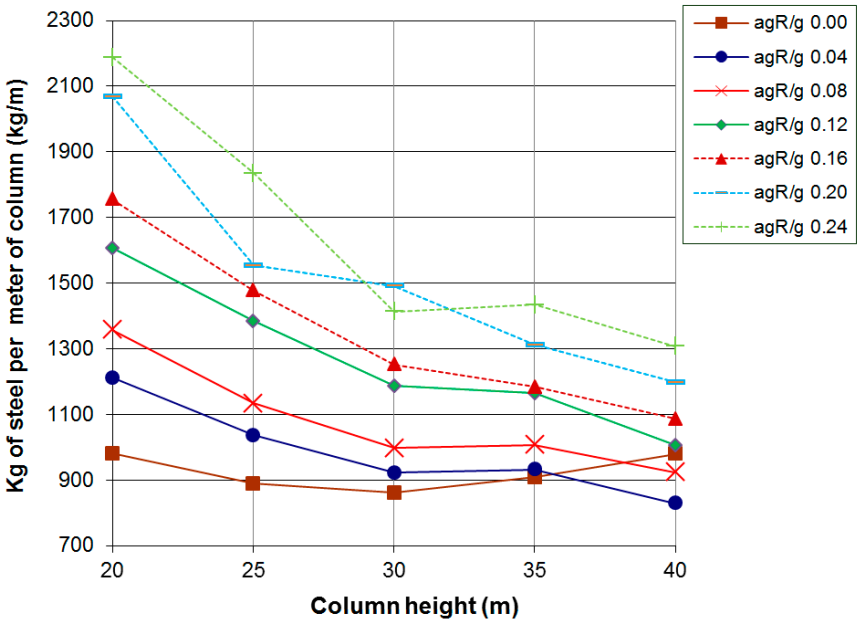

Figure 15. Water tank total steel per unit height of the column.

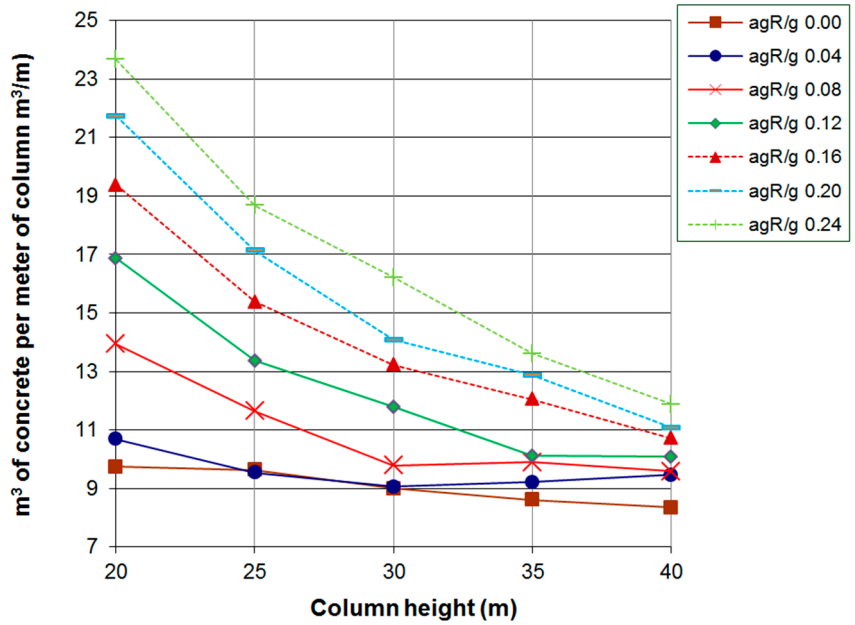

Figure 16. Water tank volume of concrete per unit height of the column.

Figure 17 shows the total cost per unit height of the 35 water tanks. Tendencies are as shown in Figures 15 and 16 since the total cost is proportional to the materials used in the water tanks. The maximum cost is 8814.80 €/m for a_{gR}/g, equal to 0.24, and a column height of 20 m. The minimum cost is 3749.51 €/m for a_{gR}/g, equal to 0.00, and a column height of 40 m. Note that costs are per unit height of the water tanks.

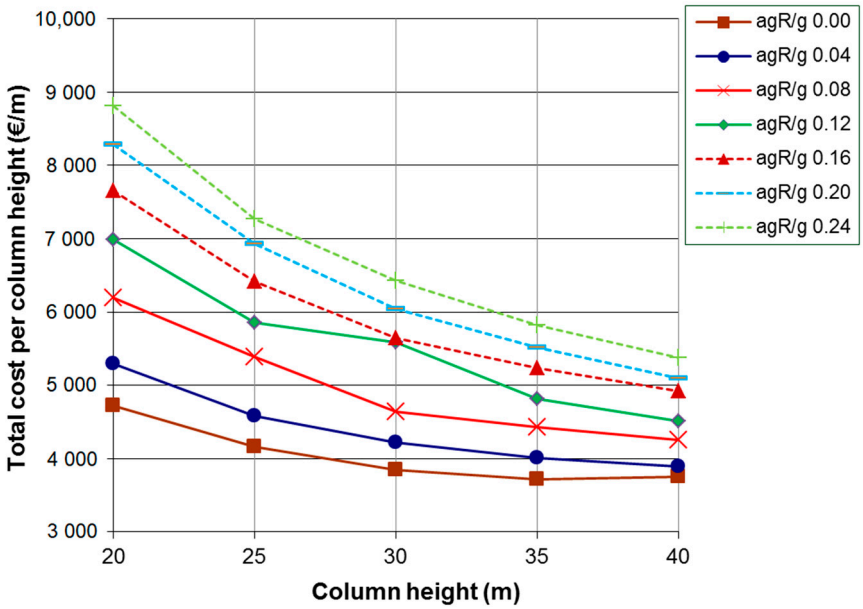

Figure 17. Water tanks total cost per unit height.

5. Concluding Remarks

35 RC elevated water tanks with a constant top reservoir were optimized. The height of the columns varied from 20 to 40 m in steps of 5 m. The seismic exposure a_{gR}/g varied from 0.00 to 0.24 in steps of 0.04. The foundation considered was a shallow RC footing with double symmetry. The foundation ground consisted of sands with an internal friction angle of 35° and no cohesion. The specific weight of the ground was 20 kN/m^3, and the SPT was equal to 30. The water table considered was sufficiently deep not to alter the foundation conditions. Columns considered were RC square hollow sections with double geometry. The shape of the constant reservoir considered was a conic trunk. The height of the reservoir was 6 m, and the top and bottom diameters were 14 and 7 m, respectively. The optimization method considered is based on a hybrid OBA strategy with mutation operators named OBAMO. This method adjusts the search for new solutions as a function of the degree of success obtained with previous solutions, which resulted in the optimal outcome for the 35 water tanks analyzed. Regarding the analysis results, it is important to note the high nonlinearity of the problem due to the interaction between the seismic forces and the rigidity of the columns. It is worth noting that a full tank of water is determinant for seismic exposures a_{gR}/g higher than 0.04. The amount of steel reinforcement and volume of concrete per unit height keeps relatively constant with the height for seismic zones of high degrees. Water tanks under no seismic conditions require more materials with height. Note also that the use of equivalent horizontal forces by the Eurocode 8 and the approximate method of Housner yield similar results. The study shows the algorithm's applicability to the structure and provides engineers with guidelines for efficient design. The results provide information for a day-to-day design of RC elevated tanks.

Author Contributions: Conceptualization, F.J.M.-M., V.Y. and A.H.; methodology, F.J.M.-M., V.Y. and A.H.; software, F.J.M.-M. and J.A.; validation, F.J.M.-M., A.H. and J.A.; formal analysis, F.J.M.-M., F.G.-V. and A.H.; investigation, F.J.M.-M., V.Y., F.G.-V. and A.H.; resources, V.Y.; data curation, F.J.M.-M. and J.A.; writing—original draft preparation, F.J.M.-M.; writing—review and editing, V.Y. and F.G.-V.;

visualization, F.G.-V. and J.A.; supervision, V.Y., F.G.-V. and A.H.; project administration, V.Y.; funding acquisition, V.Y. All authors have read and agreed to the published version of the manuscript.

Funding: Grant PID2020-117056RB-I00 funded by MCIN/AEI/10.13039/501100011033 and by "ERDF A way of making Europe".

Institutional Review Board Statement: Not applicable.

Informed Consent Statement: Not applicable.

Data Availability Statement: Not applicable.

Acknowledgments: The authors would like to thank the editor of the applied sciences and the anonymous reviewers for contributing to improve the earlier version of this manuscript.

Conflicts of Interest: The authors declare no conflict of interest.

References

1. Steinbrugge, K.V.; Rodrigo, F.A. The Chilean earthquakes of May 1960: A structural engineering viewpoint. *Bull. Seismol. Soc. Am.* **1963**, *53*, 225–307. [CrossRef]
2. Rai, D.C. Elevated tanks. *Earthq. Spectra* **2002**, *18*, 279–295. [CrossRef]
3. Zhao, C.F.; Yu, N.; Mo, Y.L. Seismic fragility analysis of AP1000 SB considering fluid-structure interaction effects. *Structures* **2020**, *23*, 103–110. [CrossRef]
4. Dilena, M.; Dell'Oste, M.P.; Gubana, A.; Morassi, A.; Polentarutti, F.; Puntel, E. Structural survey of old reinforced concrete elevated water tanks in an earthquake-prone area. *Eng. Struct* **2021**, *234*, 111947. [CrossRef]
5. Housner, G.W. The dynamic behavior of water tanks. *Bull. Seismol. Soc. Am.* **1963**, *53*, 381–389. [CrossRef]
6. Kangda, M.Z. An approach to finite element modeling of liquid storage tanks in ANSYS: A review. *Innov. Infrastruct. Solut.* **2021**, *6*, 226. [CrossRef]
7. Zhou, J.W.; Zhao, M. Shaking table test of liquid storage tank with finite element analysis considering uplift effect. *Struct. Eng. Mech.* **2021**, *77*, 369–381. [CrossRef]
8. Waghmare, M.V.; Madhekar, S.N.; Matsagar, V.A. Performance of RC elevated liquid storage tanks installed with semi-active pseudo-negative stiffness dampers. *Struct. Control Health Monit.* **2022**, *29*, e2924. [CrossRef]
9. Ghateh, R.; Kianoush, M.R.; Pogorzelski, W. Response modification factor of elevated water tanks with reinforced concrete pedestal. *Struct. Infrastruc. Eng.* **2016**, *12*, 936–948. [CrossRef]
10. Livaoglu, R. Soil interaction effects on sloshing response of the elevated tanks. *Geomech. Eng.* **2013**, *5*, 283–297. [CrossRef]
11. Mansour, A.M.; Kassem, M.M.; Nazri, F.M. Seismic vulnerability assessment of elevated water tanks with variable staging pattern incorporating the fluid-structure interaction. *Structures* **2021**, *34*, 61–77. [CrossRef]
12. El Ansary, A.M.; El Damatty, A.A.; Nassef, A.O. A coupled finite element genetic algorithm technique for optimum design of steel conical tanks. *Thin. Walled. Struct.* **2010**, *48*, 260–273. [CrossRef]
13. Stanton, A.; Javadi, A.A. An automated approach for an optimised least cost solution of reinforced concrete reservoirs using site parameters. *Eng. Struct.* **2014**, *60*, 32–40. [CrossRef]
14. Hernández, S.; Fontan, A.N.; Díaz, J.; Marcos, D. VTOP. An improved software for design optimization of prestressed concrete beams. *Adv. Eng. Softw.* **2010**, *41*, 415–421. [CrossRef]
15. Carbonell, A.; González-Vidosa, F.; Yepes, V. Design of reinforced concrete road vaults by heuristic optimization. *Adv. Eng. Softw.* **2011**, *42*, 151–159. [CrossRef]
16. Medeiros, G.F.; Kripka, M. Modified harmony search and its application to cost minimization of RC columns. *Adv. Compt. Des.* **2017**, *2*, 1–13. [CrossRef]
17. Molina-Moreno, F.; García-Segura, T.; Martí, J.V.; Yepes, V. Optimization of buttressed earth-retaining walls using hybrid harmony search algorithms. *Eng. Struct.* **2017**, *134*, 205–216. [CrossRef]
18. García-Segura, T.; Penadés-Plà, V.; Yepes, V. Sustainable bridge design by metamodel-assisted multi-objective optimization and decision-making under uncertainty. *J. Clean. Prod.* **2018**, *202*, 904–915. [CrossRef]
19. García, J.; Martí, J.; Yepes, V. The Buttressed Walls Problem: An Application of a Hybrid Clustering Particle Swarm Optimization Algorithm. *Mathematics* **2020**, *8*, 862. [CrossRef]
20. Taiyari, F.; Kharghani, M.; Hajihassani, M. Optimal design of pile wall retaining system during deep excavation using swarm intelligence technique. *Structures* **2020**, *28*, 1991–1999. [CrossRef]
21. Negrín, I.A.; Chagoyén, E.L. Economic and environmental design optimisation of reinforced concrete frame buildings: A comparative study. *Structures* **2022**, *38*, 64–75. [CrossRef]
22. Zhuang, X.; Zhou, S. The prediction of self-heating capacity of bacteria-based concrete using machine learning approaches. *Comput. Mater Contin.* **2019**, *59*, 57–77. [CrossRef]
23. Ramezani, M.; Kim, Y.H.; Sun, Z. Modeling the mechanical properties of cementitious materials containing CNTs. *Cem. Concr. Compos.* **2019**, *104*, 103347. [CrossRef]

24. Ramezani, M.; Kim, Y.H.; Sun, Z. Probabilistic model for flexural strength of carbon nanotube reinforced cement-based materials. *Compos. Struct.* **2020**, *253*, 112748. [CrossRef]
25. Lopes Silva, M.A.; de Souza, S.R.; Souza, M.J.F.; de Franca, M.F. Hybrid metaheuristics and multi-agent systems for solving optimization problems: A review of frameworks and a comparative analysis. *Appl. Soft. Comput.* **2018**, *71*, 433–439. [CrossRef]
26. Martínez, F.J.; González-Vidosa, F.; Hospitaler, A.; Yepes, V. Heuristic optimization of RC bridge piers with rectangular hollow sections. *Comput. Struct.* **2010**, *88*, 375–386. [CrossRef]
27. Penadés-Plà, V.; García-Segura, T.; Yepes, V. Accelerated optimization method for low-embodied energy concrete box-girder bridge design. *Eng. Struct.* **2019**, *179*, 556–565. [CrossRef]
28. Mathern, A.; Penadés-Plà, V.; Barros, J.A.; Yepes, V. Practical metamodel-assisted multi-objective design optimization for improved sustainability and buildability of wind turbine foundations. *Struct. Multidiscipl. Optim.* **2022**, *65*, 46. [CrossRef]
29. Tu, J.; Zhang, Y.; Mei, G.; Xu, N. Numerical investigation of progressive slope failure induced by sublevel caving mining using the finite difference method and adaptive local remeshing. *Appl. Sci.* **2021**, *11*, 3812. [CrossRef]
30. Zhou, S.; Zhu, H.; Yan, Z.; Ju, J.W.; Zhang, L. A micromechanical study of the breakage mechanism of microcapsules in concrete using PFC2D. *Const. Build. Mater.* **2016**, *115*, 452–463. [CrossRef]
31. Eurocode 2. *Design of Concrete Structures. Part 1–1: General Rules and Rules for Buildings*; European Committee for Standardization: Brussels, Belgium, 2004.
32. Ministerio Presidencia. *Code of Structures*; Ministerio Presidencia: Madrid, Spain, 2021.
33. Eurocode 8. *Design of Structures for Earthquake Resistance—Part 1: General Rules, Seismic Actions and Rules for Buildings*; European Committee for Standardization: Brussels, Belgium, 2004.
34. Ministerio de Fomento. *Technical Building Code Part II. Basic Document SE-AE, Structural Safety. Building Actions*; Ministerio de Fomento: Madrid, Spain, 2009.
35. Eurocode 1. *Basis of Design and Actions on Structures. Part 1: General Actions and Part 4: Silos and Tanks*; European Committee for Standardization: Brussels, Belgium, 2003.
36. Hansen, J.B. A General Formula for Bearing Capacity. *Dan. Geotech. Inst. Bull.* **1961**, *11*, 38–46.
37. Hansen, J.B. A Revised and Extended Formula for Bearing Capacity. *Dan. Geotech. Inst. Bull.* **1970**, *28*, 5–11.
38. Burland, J.B.; Burbidge, M.C. Settlement of foundations on sand and gravel. *Proc. Inst. Civil. Eng. Civ. Eng.* **1985**, *78*, 1325–1381. [CrossRef]
39. Bonet, J.L.; Romero, M.L.; Miguel, P.F.; Fernández, M.A. A fast stress integration algorithm for reinforced concrete sections with axial loads and biaxial bending. *Comput. Struct.* **2004**, *82*, 213–225. [CrossRef]
40. Hu, T.C.; Kahng, A.B.; Tsao, C.W.A. Old bachelor acceptance: A new class of nonmonotone threshold accepting methods. *ORSA J. Comput.* **1995**, *7*, 417–425. [CrossRef]
41. Agur, Z.; Hassin, R.; Levy, S. Optimizing chemotherapy scheduling using local search heuristics. *Oper. Res.* **2006**, *54*, 829–846. [CrossRef]
42. Luz, A.; Yepes, V.; González-Vidosa, F.; Martí, J.V. Design of open reinforced concrete abutments road bridges with hybrid stochastic hill climbing algorithms. *Inf. Constr.* **2015**, *67*, e114.
43. Yepes, V.; Martí, J.V.; García-Segura, T.; González-Vidosa, F. Heuristics in optimal detailed design of precast road bridges. *Arch. Civ. Mech. Eng.* **2017**, *17*, 738–749. [CrossRef]
44. Yepes, V.; Dasí-Gil, M.; Martínez-Muñoz, D.; López-Desfilís, V.J.; Martí, J.V. Heuristic techniques for the design of steel-concrete composite pedestrian bridges. *Appl. Sci.* **2019**, *9*, 3253. [CrossRef]
45. Martínez-Muñoz, D.; Martí, J.V.; García, J.; Yepes, V. Embodied energy optimization of buttressed earth-retaining walls with hybrid simulated annealing. *Appl. Sci.* **2021**, *11*, 1800. [CrossRef]
46. Martínez-Martín, F.J.; González-Vidosa, F.; Hospitaler, A.; Yepes, V. A parametric study of optimum tall piers for railway bridge viaducts. *Struct. Eng. Mech.* **2013**, *45*, 723–740. [CrossRef]